Cancer Gene Therapy (2012) 19, 508 – 516

www.nature.com/cgt

ORIGINAL ARTICLE

Interferon-β lipofection I. Increased efficacy of chemotherapeutic drugs on human tumor cells derived monolayers and spheroids

MS Villaverde, ML Gil-Cardeza, GC Glikin and LME Finocchiaro

We evaluated the effect of *hIFNβ* gene transfer alone or in combination with different antineoplastic drugs commonly used in cancer treatment. Five human tumor-derived cell lines were cultured as monolayers and spheroids. Four cell lines (Ewing sarcomas EW7 and COH, melanoma M8 and mammary carcinoma MCF-7) were sensitive to *hIFNβ* gene lipofection. Although this effect appeared in both culture configurations, spheroids showed a relative multicellular resistance (insensitive colon carcinoma HT-29 excluded). EW7 and M8 hIFNβ-expressing cells were exposed to different concentrations of bleomycin, bortezomib, carboplatin, doxorubicin, etoposide, methotrexate, paclitaxel and vincristine in both configuration models. In chemotherapy-sensitive EW7 monolayers, the combination of *hIFNβ* gene and antineoplastic drugs displayed only additive or counteractive (methotrexate) effects, suggesting that cytotoxic mechanisms triggered by *hIFNβ* gene lipofection could be saturating the signaling pathways. Conversely, in chemotherapy-resistant EW7 spheroids or M8 cells, the combination of *hIFNβ* with drugs that mainly operate at the genotoxic level (doxorubicin, methotrexate and paclitaxel) presented only additive effects. However, drugs that also increase pro-oxidant species can complement the antitumor efficacy of the *hIFNβ* gene and clearly caused potentiated effects (bleomycin, bortezomib, carboplatin, etoposide and vincristine). The great bystander effect induced by *hIFNβ* gene lipofection could be among the main causes of its effectiveness, because only 1 or 2% of EW7 or M8 hIFNβ-expressing cells killed more than 60 or 80% of cell population, respectively.

Cancer Gene Therapy (2012) **19,** 508–516; doi:10.1038/cgt.2012.27; published online 18 May 2012

Keywords: chemotherapy; Ewing sarcoma; interferon-β; lipofection; melanoma; spheroids

INTRODUCTION

The development of therapeutic strategies to improve overall survival in refractory advanced cancer remains a high priority. Interferons (IFNs) are well known for both their antiproliferative effects as well as their immunomodulatory activity. Being the first cytokines to be clinically applied in human cancer, their efficacies have been observed in hairy cell leukemia,[1,2] chronic myelogenous leukemia[3,4] and melanoma.[5] The combination of cytokines with other agents that display antitumor effects may result in an optimized therapy. Several comparative studies demonstrated an increased objective response rate with the addition of hIFNs compared with cytotoxic agents alone.[6–8]

Despite the demonstrated clinical effectiveness, the treatment with IFNα/β is associated with substantial systemic toxicity that worsens the patient's quality of life and often prejudices the therapy completion (about 25% of the treated patients).[5,8] In the case of hIFNβ, the direct antiproliferative effect relies on concentrations that cannot be achieved by systemic protein administration because of toxicity and rapid protein clearance.[9] Therefore, the limited performance of hIFNs in cancer trials may have been caused by the lack or insufficiency of sustained delivery of the protein to the tumor site. In a previous study, we have demonstrated that the exogenously added recombinant human IFNβ protein can be successfully replaced by the transfer of the corresponding gene *in vitro*. Local nonviral gene therapy-mediated approach for the delivery of this cytokine may have the potential to overcome the above-mentioned limitations, and may allow taking advantage of IFNα/β effectiveness without the currently associated undesirable side effects.[10–12]

Gene therapy has been proposed as a strategy to enhance the antitumor effect of drugs in the treatment of refractory or advanced cancers. The combined use of gene therapy and cytotoxic drugs has been reported in bladder,[13,14] pancreatic,[15] colorectal[16] and breast[17] cancer. In addition, an increasing number of studies have recently shown that immunogene therapy is not only compatible with, but may also be synergistic with certain chemotherapies.[18] Then, more studies to explore the combined use of these two modalities are thus needed.

We have previously developed a three-dimensional (3D) spheroid cell culture model, which better represent the anchorage-independent *in vivo* setting of tumor cells than monolayers. The morphological and biochemical characteristics of spheroid tumor cells closely resemble those of primary tumors.[19] Thus, the *in vitro* response of tumor-derived spheroids (but not the corresponding monolayers) correlated with the clinical outcome of the suicide gene treatment observed on canine melanoma patients *in vivo*.[20]

The aim of this study was to evaluate whether the *hIFNβ* gene improved the antitumor effect of antineoplastic drugs used as first-line treatment in the management of advanced cancer.

Our results clearly showed a strongly enhanced tumor cell growth inhibition by combining *hIFNβ* gene transfer with antineoplastic drugs that, besides being genotoxic, increase reactive oxygen species concentration, especially when tumor cells exhibit a

Unidad de Transferencia Genética, Instituto de Oncología 'Ángel H. Roffo', Universidad de Buenos Aires, Buenos Aires, Argentina. Correspondence: Dr LME Finocchiaro, Unidad de Transferencia Genética, Instituto de Oncología 'Ángel H. Roffo', Universidad de Buenos Aires, Av. San Martín 5481, 1417 Buenos Aires, Capital Federal, Argentina.
E-mail: gglikin@bg.fcen.uba.ar
Received 18 August 2011; revised 22 March 2012; accepted 18 April 2012; published online 18 May 2012

chemo-resistant phenotype as EW7 Ewing sarcoma spheroids or M8 melanoma in both spatial configurations.

MATERIALS AND METHODS

Cell cultures

Human Ewing sarcoma (EW7 and COH),[21] melanoma (M8),[22] mammary carcinoma (MCF-7, ATCC# HTB-22) and colorectal adenocarcinoma (HT-29, ATCC# HTB-38) cells were cultured as monolayers at 37 °C in a humidified atmosphere of 95% air and 5% CO_2 with DMEM/F12 medium (Invitrogen, Carlsbad, CA) containing 10% FBS (Invitrogen), 10 mM HEPES (pH 7.4) and antibiotics. Serial passages were done by trypsinization (0.25% trypsin and 0.02% EDTA in phosphate-buffered saline) of subconfluent monolayers.

Plasmids

Plasmids psCMVβ and psCMV-*hIFN*β were built replacing the HSV thymidine kinase gene of psCMV*tk*[23] by *Escherichia coli* β-galactosidase (*βgal*)[24] and *hIFN*β genes, respectively. Plasmids were amplified in *E. coli* DH5α (Invitrogen), grown in LB medium containing 100 μg ml^{-1} neomycin and purified by ion-exchange chromatography (Qiagen, Valencia, CA).

Liposome preparation and *in vitro* lipofection

DC-Chol (3β[N-(*N*′,*N*′-dimethylaminoethane)-carbamoyl] cholesterol) and DMRIE (1,2-dimyristyloxypropyl-3-dimethyl-hydroxyethilammonium bromide) were synthesized, and were kindly provided by BioSidus (Buenos Aires, Argentina). DOPE (1,2-dioleoyl-*sn*-glycero-3-phosphatidyl ethanolamine) was purchased from Sigma (St Louis, MO). Liposomes were prepared at lipid/co-lipid molar ratios of 3:2 (DC-Chol/DOPE) or 1:1 (DMRIE/DOPE) by sonication as described.[25,26] Optimal lipid mixtures were determined for every cell line.[20]

Cultured cells at a density of 5×10^4 cells per cm^2 (about 40% confluence) were exposed to lipoplexes (1 μl liposomes per cm^2 and 0.5 μg DNA per cm^2) during 4–6 h.[20]

β-Galactosidase staining

To measure gene transfer efficiency, psCMVβ lipofected cells were trypsinized, fixed in suspension, stained with 5-bromo-4-chloro-3-indolyl β-D-galactopyranoside (Sigma) and counted using an inverted phase-contrast microscope.[19]

Sensitivity to hIFNβ assay

Twenty-four hours after lipofection, transiently hIFNβ- or βgal-expressing cells were seeded on regular plates as monolayers or on top of 1.5% solidified agar to form spheroids (5.0×10^4 cells per ml and 2.0×10^5 cells per ml, respectively). Then cells were incubated for 5 days in monolayers or 9 days in spheroids. Cell viability was quantified using a colorimetric CellTiter 96 Aqueous Non radioactive MTS Cell Proliferation Assay according to the manufacturer's instructions (Promega, Madison, WI). The percentage of cell survival was calculated referring to control as 100% of survival.

Sensitivity to chemotherapeutic drugs assays

To determine the effect of the combined therapy, EW7 and M8 non-lipofected and lipofected cells were exposed to bleomycin (BLM; Gador, Buenos Aires, Argentina), bortezomib (BTZ; Janssen, Buenos Aires, Argentina), carboplatin (CBP; Aspen, Buenos Aires, Argentina), doxorubicin (DXR; Aspen), etoposide (ETP, Sigma), methotrexate (MTX; LKM, Buenos Aires, Argentina), paclitaxel (PTX; Aspen) and vincristine (VCN; LKM) at different concentrations, 24 h after lipofection and then incubated for 5 days (monolayers) or 9 days (spheroids). The growth inhibitory effect of *hIFN*β gene and/or drugs was assessed by MTS (Promega) or acid phosphatase (see below) assay.

Acid phosphatase assay

The acid phosphatase assay was performed as reported.[27] Briefly, spheroids growing in liquid overlay were transferred to 96-well microplates, washed and finally treated with 100 μl of the assay buffer (0.1 M sodium acetate, 0.1% Triton X-100, supplemented with *p*-nitrophenyl phosphate) per well and incubated for 90 min at 37 °C. Following incubation, 10 μl of 1 N NaOH was added to each well, and absorption at 405 nm was measured within 10 min.

Spheroids volume measurement

The average diameter of spheroids was recorded as measure of two diameters under an inverted microscope. Results were expressed as mean (of a minimum of 15 spheroids diameters) ± s.e.m. ($n = 4$ independent assays).

Protein determinations

Protein concentrations were determined by the method of Bradford.[28]

Statistics

Results were expressed as mean ± s.e.m. (*n*: number of experiments corresponding to independent assays). Differences between groups were determined by analysis of variance.

RESULTS

Lipofection with *hIFN*β gene displayed a strong cytotoxic effect on tumor cells

In order to establish the feasibility of a nonviral gene therapy achieved by lipoplexes carrying the *hIFN*β gene, we lipofected human cell lines derived from different kinds of tumors (EW7, COH: Ewing sarcomas; M8: melanoma; MCF-7: mammary adenocarcinoma; HT-29: colon adenocarcinoma) grown as monolayers or spheroids as shown in Figure 1.

EW7, COH and M8 were able to assemble stable single spheroids when growing on agar-coated wells. While EW7 and COH spheroids were bigger (about 1.5 mm^3) and highly compact, M8 spheroids adopted a smaller (about 0.5 mm^3) and looser structure. Neither MCF-7 nor HT-29 cells were able to form single spheroids under our culture conditions.

While viability of βgal-expressing EW7, COH, M8 and HT-29 ranged from 75 to 95%, in the case of MCF-7 it was only 45%, possibly because lipoplex treatment stimulated the expression and release of IFNβ.[29] The transfer of *hIFN*β gene caused an additional strong cell viability inhibition (about 50%) in EW7, COH, MCF-7 and M8. This additional effect was only slight in HT-29 (Figure 1).

Spheroids displayed multicellular resistance to *hIFN*β transgene expression

Multicellular spheroids represent a highly valuable *in vitro* tumor model to explore how the spatial configuration of cells could affect the efficacy of *hIFN*β gene therapy under conditions that more closely resemble the *in vivo* situation.[20] When cultured as spheroids, most of the assayed cell lines (HT-29 excluded) manifested a relative *hIFN*β gene resistance phenotype, compared to the same cells grown as sparse monolayer cultures (Figure 1). This decrease of sensitivity implies the presence of the phenomenon called multicellular resistance (MCR), which can be quantified as MCR index (MCRi) and calculated as follows: MCRi = (% spheroid viability − % monolayer viability)/% monolayer viability.[20] M8 melanoma cells displayed the highest MCRi, followed by MCF-7, COH and EW7. The weakly sensitive HT-29 displayed the lowest MCRi (Table 1).

Taking into account the low lipofection efficiencies of Ewing and melanoma cells (Table 1), this outcome was very encouraging. The high bystander effect induced by *hIFN*β gene lipofection could be the main cause of its effectiveness. Even though only 0.8% of EW7 and COH cells expressed detectable amounts of the gene, this effect destroyed more than 60 and 40% of the two-dimensional (2D)- and 3D-cultured cells, respectively. Furthermore, the presence of 2.0% *hIFN*β-lipofected M8 cells was sufficient to

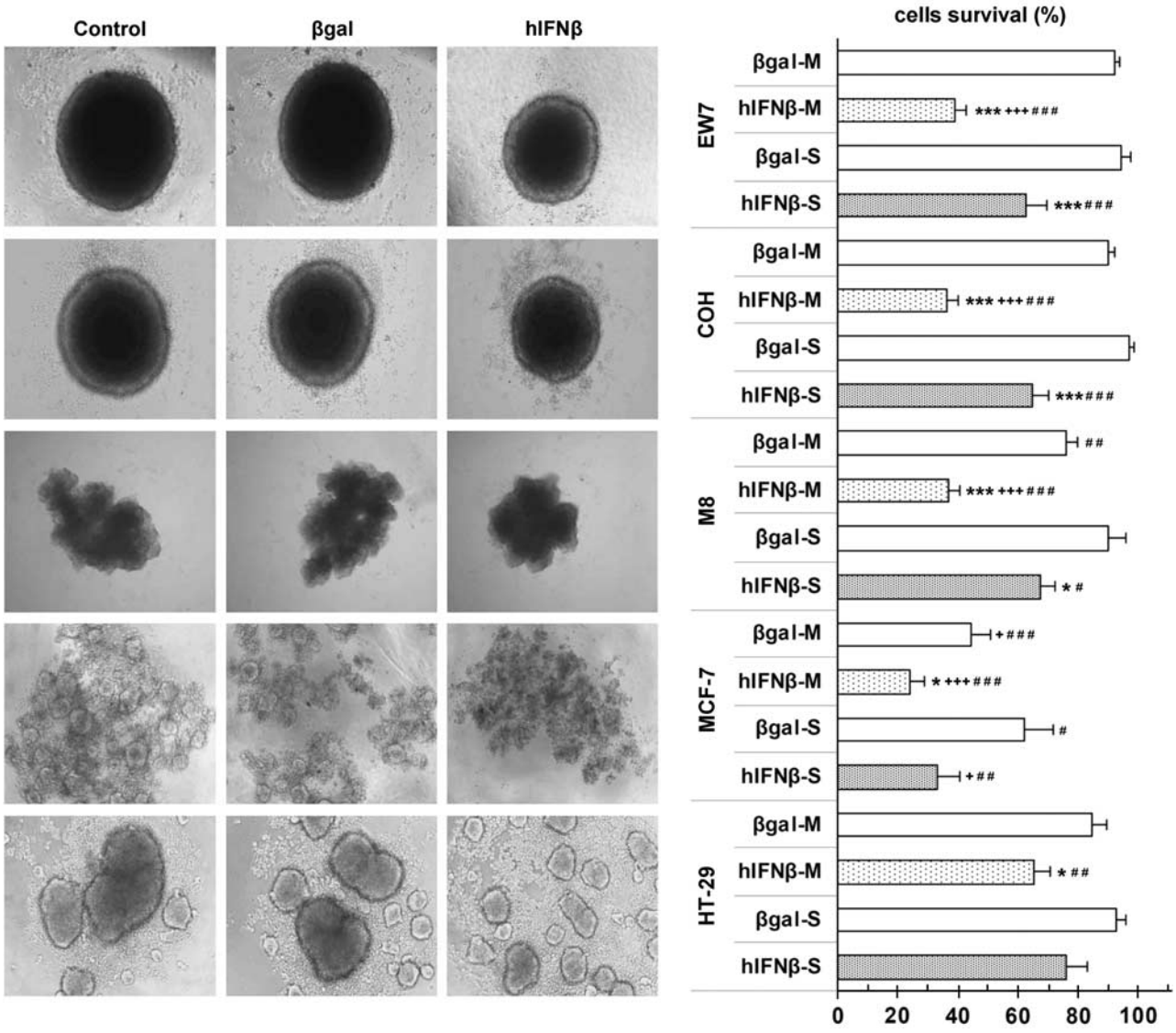

Figure 1. Cytotoxic effects of *hIFNβ* lipofection on monolayers (M) and spheroids (S). Transiently β-galactosidase (*βgal*)- or *hIFNβ*-lipofected EW7, COH, M8, MCF-7 and HT-29 cells were cultured as monolayers or spheroids and cell viability was quantified by MTS on day 5, as described in Materials and methods. Results are expressed as means ± s.e.m of $n > 4$ independent experiments. $^{***}P < 0.001$, $^{*}P < 0.05$ with respect to *βgal*; $^{\#\#\#}P < 0.001$ and $^{\#\#}P < 0.01$ with respect to control; $^{\#}P < 0.05$ with respect to control; $^{+++}P < 0.001$ and $^{+}P < 0.05$ with respect to *hIFNβ* lipofected HT-29.

Table 1. Monolayers lipofection efficiencies and spheroid MCRi to *hIFNβ*

Cell line	*Lipofection efficiency (%)*	*MCRi (%)*
EW7	0.80 ± 0.09	0.59
COH	0.81 ± 0.10	0.78
M8	1.99 ± 0.31	1.05
MCF-7	18.18 ± 3.96	0.88
HT-29	3.54 ± 1.16	0.18

Abbreviation: MCRi, multicellular resistance index.
Lipofection efficiencies were determined as described in Materials and methods. MCRi values were calculated from the results displayed in Figure 1 as described.[20]

induce a powerful bystander effect that killed 60 and 35% of the corresponding 2D- and 3D cultures, respectively (Figure 1). The bystander effect was weaker for MCF-7 and HT-29 cells. Eighteen percent of *hIFNβ*-lipofected MCF-7 cells destroyed 60 and 40% of the 2D- and 3D-cultured cells, respectively. In the case of *hIFNβ*-lipofected HT-29 cells, 3.5% of them destroyed 35% of the 2D cultures, without any effect on 3D-growing cells (Figure 1).

Despite the relative resistance displayed by tumor cells growing in 3D configuration, the lipofection with *hIFNβ* induced a spheroid size decrease in most of the tested tumor cell lines (HT-29 excluded), with a concomitant spheroid morphological change (Figure 1, left panels) and decrease of cellular viability (Figure 1, right panel).

To confirm that lipofection with *hIFNβ* gene did not primarily affect the spheroid assembly, 3-day-old EW7 spheroids were lipofected and their growth evaluated at day 12. As shown in Figure 2 and Table 2, spheroid growth (measured as volume) was significantly inhibited as compared with nonlipofected or *βgal*-lipofected controls, indicating that either lipofection/assembly or assembly/lipofection yielded similar results. For the sake of simplicity, in further experiments, lipofection was performed at day 0, preceding spheroid assembly.

hIFNβ lipofection modified chemotherapy effects on both EW7 and M8 monolayers

Simultaneous attack of different therapeutic targets often constitutes an effective strategy for the treatment of the oncologic patient. In this way, it is reasonable to investigate if *hIFNβ* gene therapy can be successfully combined with antineoplastic drugs frequently used in the clinical practice as BLM, BTZ, CBP, DXR, ETP, MTX, PTX and VCN.

For the sake of simplicity, we assayed EW7 and M8 cell lines that displayed different sensitivities to chemotherapy, cultured as monolayers and spheroids. As it was mentioned above, both cell lines resulted significantly sensitive to *hIFNβ* gene transfer. For every drug treatment seen in Figure 3, monolayer survival was expressed as percentage of the untreated cells (left plots) or the corresponding cells without antineoplastic drug (right plots).

M8 monolayers lipofected with *hIFNβ* lost 70–80% of viability. Even if it resulted less sensitive than M8 to *hIFNβ* lipofection, EW7 displayed 50–60% of cell viability inhibition (Figure 3, see *Y* axes). EW7 monolayers were always more sensitive than M8 to increasing concentrations of antineoplastic drugs. In EW7 cells, drugs alone decreased from 5 to 45% of cell viability, while the *hIFNβ* gene lipofection drastically increased the drugs antitumor effect to 70–90% ($P<0.01$).

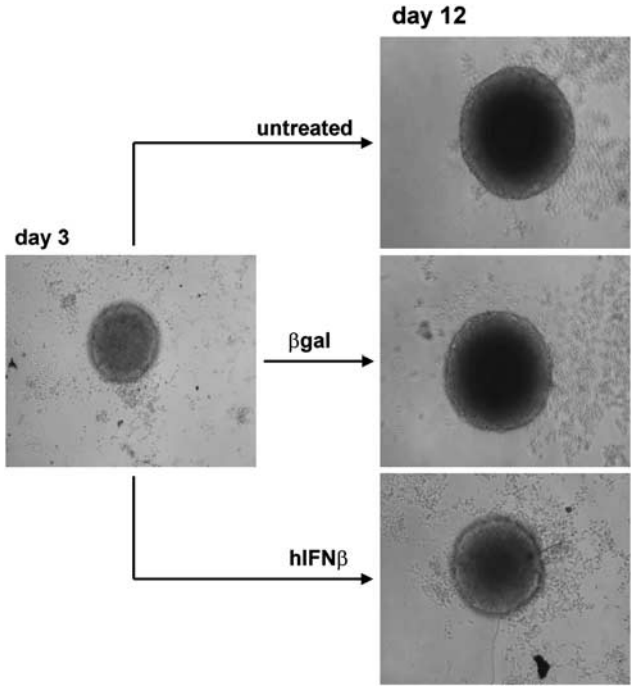

Figure 2. Direct lipofection of EW7 spheroids. Cells were cultured as spheroids for 3 days and split into three groups. A portion remained untreated, other portions were lipofected with β-galactosidase (*βgal*) or with *hIFNβ* gene, as described in Materials and methods. Then spheroids were cultured for additional 9 days. Images represent individual spheroids ($n>4$) growing in 96-well plates.

As seen in Figure 3, left plots, at the pharmacologically relevant concentrations used for spheroids treatment (see legends to Figures 4 and 5), drugs alone decreased cell viability in M8 monolayers from 0.5 to 34% (PTX excluded), whereas drugs combined with the *hIFNβ* gene lipofection drastically increased its antitumor effect from 81 to 96% ($P<0.01$). Lipofection with *βgal* gene caused 0–10% loss of cell viability in the absence of drugs, but it increased drug sensitivity in EW7 and M8 monolayers. As seen in Figure 3, right plots, lipoplex-sensitive M8 cell line displayed *βgal* left shifted curves for BLM, BTZ, DXR, MTX, PTX and VCN. EW7 monolayers also showed a slight left shift for VCN. This enhanced drug effect of unspecific lipofection was caused by the pDNA/cationic lipid complex, as the addition of free cationic lipids did not potentiate the drugs antitumor effect (data not shown). Given that cellular uptake of drugs may depend on active transport, it is conceivable that lipofection helped this process in M8 cells. This phenomenon is currently under study in our laboratory (Gil-Cardeza *et al*., personal communication).

As deduced from the IC_{50}s (Table 3), nonlipofected EW7 cells were more sensitive than M8 to CBP (10-fold), MTX (15-fold), ETP (20-fold) and VCN (30-fold).

In EW7, lipoplexes carrying *hIFNβ* gene shifted the curves for CBP and ETP slightly to the left, with respect to *βgal* controls. Surprisingly, *hIFNβ* lipofection shifted the MTX curve to the right, indicating a clear counteractive effect (Figure 3, right plot).

In general, the *hIFNβ* enhancing effects appeared in M8 cells that were more sensitive to *hIFNβ* gene treatment and less sensitive to chemotherapeutic drugs. As seen in Figure 3, right columns, in the presence of the *hIFNβ* gene, BLM, BTZ, CBP and VCN shifted their dose–response curves to the left, indicating strongly enhanced effects for the gene/chemotherapy combination.

hIFNβ lipofection improved chemotherapy effects on both EW7 and M8 multicellular spheroids

To confirm the effectiveness of *hIFNβ* lipofection/drugs combined therapy in Ewing cancer and melanoma cells, we used spheroids from these cells as an experimental system that mimics the real biological environment of a tumor, including limitations in drug or gene penetration[30] and distribution and feedback mechanisms in cell signaling.[31]

The single-spheroid model produced by EW7 and M8 cells in agar-coated 96-well plates is a very useful model because of the simplicity of measuring the spheroids radii to calculate volumes. Although size and total protein measurements displayed a good correlation, in some cases the level of significance of the two methodologies differed. For the sake of simplicity of data analysis, we considered that differences were significant when they appeared in both parameters.

At the assayed concentrations, half of the drugs (CBP, DXR, MTX, VCN) displayed significant inhibitory effects compared with

Table 2. Tumor diameters and volumes of *hIFNβ*-lipofected spheroids

Treatment	*Day 3*		*Day 12*		
	Diameter (μm)	*Volume (mm^3)*	*Diameter (μm)*	*Volume (mm^3)*	*Size (%)*
Control	381 ± 2	0.0264 ± 0.0017	635 ± 2	0.1215 ± 0.0041	100
βgal	NA	NA	595 ± 1	0.0996 ± 0.0014	76
hIFNβ	NA	NA	517 ± 4	0.0658 ± 0.0053	41

Abbreviation: NA, not applicable.
The experiment was performed as depicted in Figure 2.

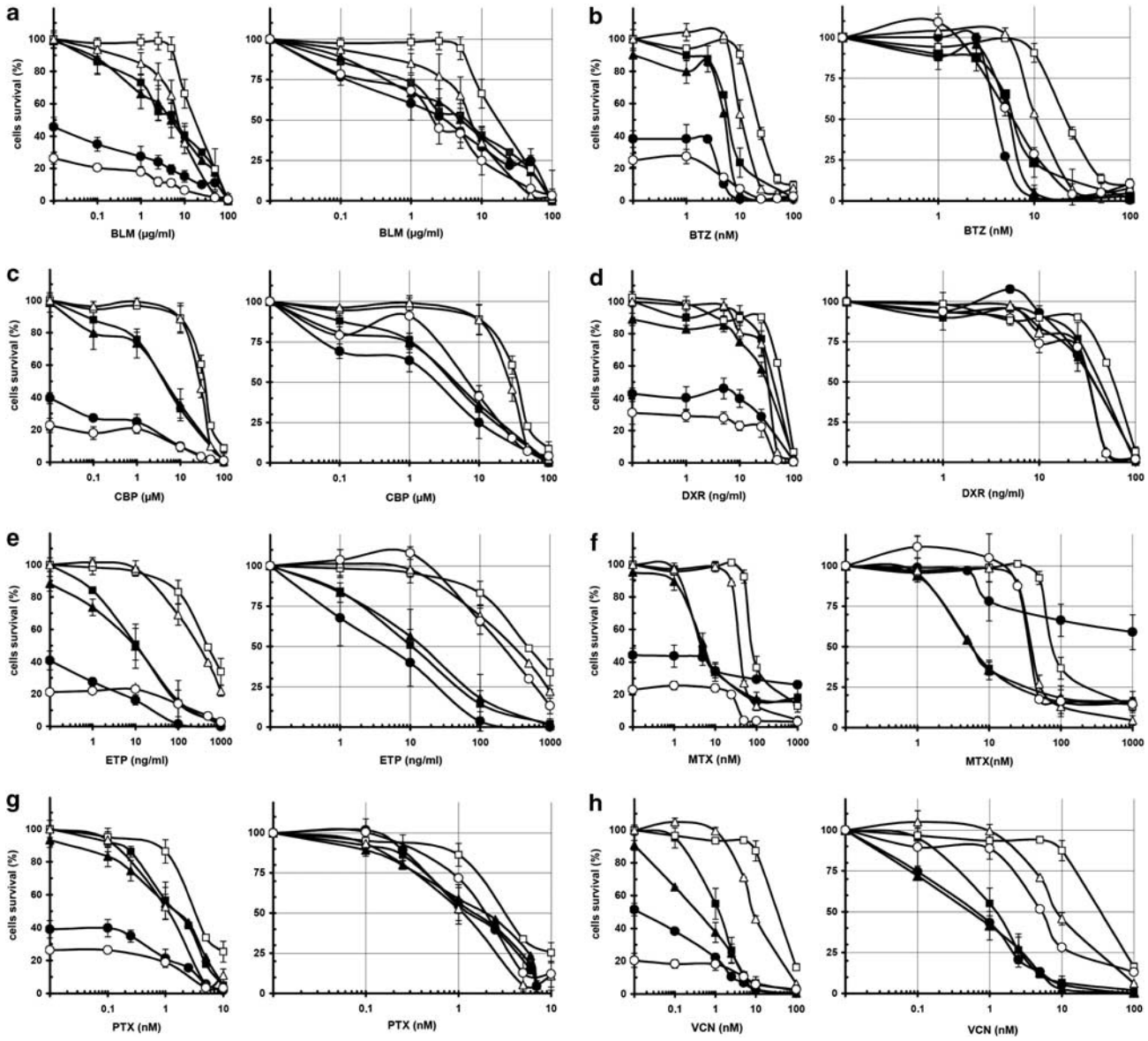

Figure 3. *In vitro* dose–response curves of antineoplastic drugs for untreated (■, □) β-galactosidase (*βgal*)-lipofected (▲, △), *hIFNβ*-ipofected (●, ○) EW7 (■, ▲, ●) and M8 (□, △, ○) monolayers. The assay was performed as described in Materials and methods. Results were expressed as mean ± s.e.m. of $n > 4$ independent experiments. Each panel displays the results as percentage of the untreated condition (no gene transfer, no drug: left plots) and as percentage of their respective gene transfer conditions (no drug: right plots). (**a**) BLM, bleomycin; (**b**) BTZ, bortezomib; (**c**) CBP, carboplatin; (**d**) DXR, doxorubicin; (**e**) ETP, etoposide; (**f**) MTX, methotrexate; (**g**) PTX, paclitaxel; and (**h**) VCN, vincristine.

unlipofected control spheroids, while the remainder (BLM, BTZ, ETP, PTX) showed nonsignificant changes. As seen in Figure 4, in the absence of antineoplastic drugs, EW7 spheroids were not sensitive to *βgal* lipofection but they were sensitive to *hIFNβ* that caused about 50% of spheroid volume loss. Even combined with antineoplastic agents, *βgal* lipofection did not significantly affect EW7 spheroid volume as compared with their respective drug-treated controls. Conversely, the combination with *hIFNβ* lipofection resulted in a significant reduction of spheroid volume as seen for almost all the assayed drugs (MTX and PTX excluded). The highest inhibitory effects were found for the combination of *hIFNβ* with BLM, BTZ, DXR, ETP and VCN as compared with drug or *hIFNβ* gene added separately. It is worth to note that EW7 spheroids were resistant to BLM, BTZ, ETP and PTX. BTZ combined with *hIFNβ* caused a characteristic and consistent morphological change of the EW7 spheroids that correlated with a decrease of their volumes.

On the other hand, additive effects of *hIFNβ* were found with CBP. In the case of PTX, which did not show a clear inhibitory effect at the assayed concentration, *hIFNβ* lipofection caused a proportion of cell death similar to the corresponding control without the drug. Only in the case of MTX, *hIFNβ* did not enhance the inhibition caused by the drug and displayed a clear counteracting effect.

The small size and looser structure of M8 spheroids allowed quantifying its cell viability by acid phosphatase assay. As shown in Figure 5, at the assayed concentrations half of the drugs displayed inhibitory effects on unlipofected control M8 spheroids (BLM, BTZ, CBP and PTX), while the remainder (DXR, ETP, MTX, VCN) showed nonsignificant changes. In the absence of antineoplastic drugs, M8 spheroids were not sensitive to *βgal* lipofection alone, but they were sensitive to *hIFNβ* that caused about 30% of spheroid volume loss. Even combined with antineoplastic agents, *βgal* lipofection did not significantly affect M8

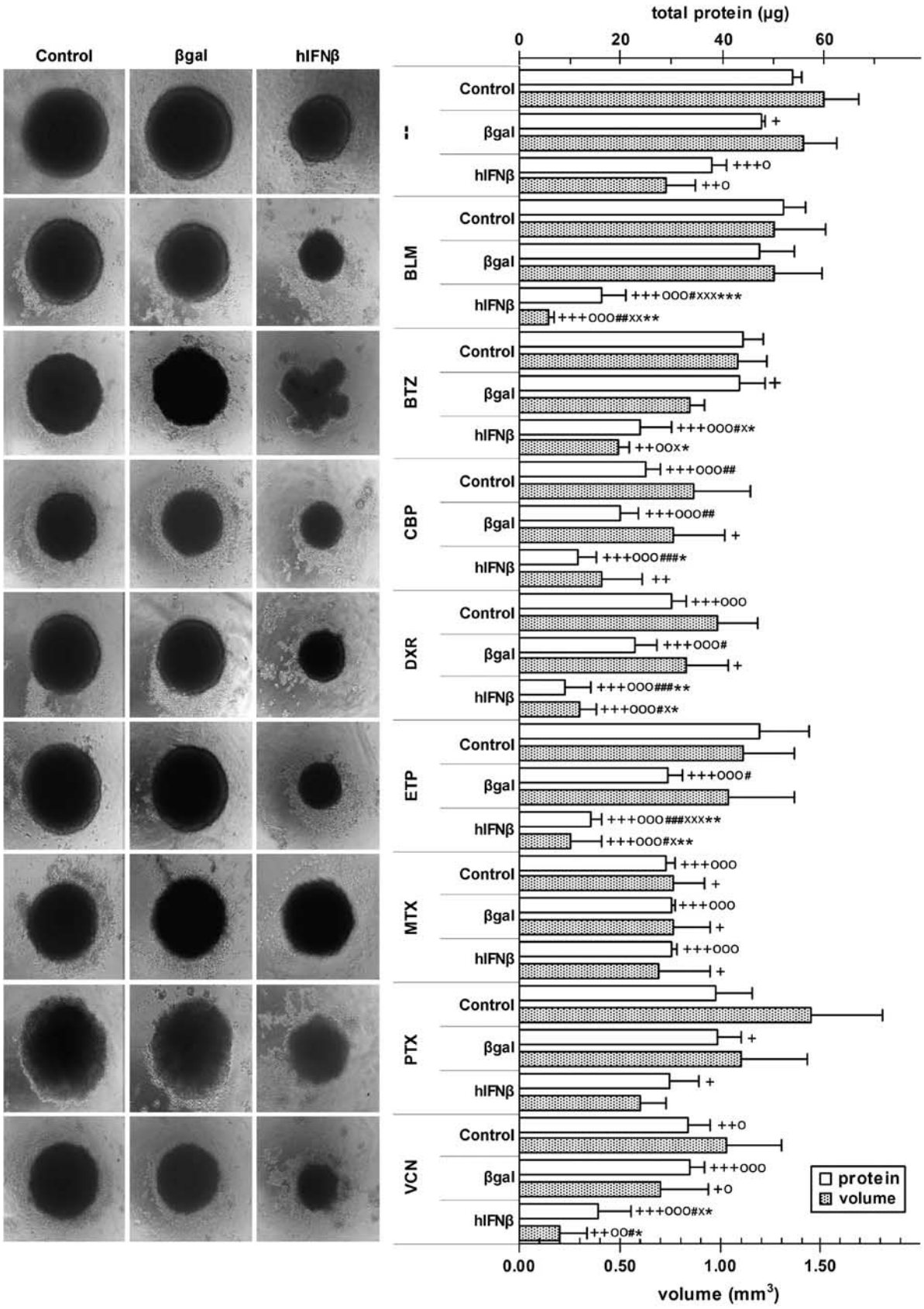

Figure 4. Responses to antineoplastic drugs for untreated (control), β-galactosidase (*βgal*)- and *hIFNβ*-lipofected EW7 spheroids. The assay was performed as described in Materials and methods. Results were expressed as mean ± s.e.m. of four independent experiments. Bleomycin (BLM 10 μg ml^{-1}), bortezomib (BTZ 10 nM), carboplatin (CBP 5 μM), doxorubicin (DXR 25 ng ml^{-1}), etoposide (ETP 50 ng ml^{-1}), methotrexate (MTX 10 nM), paclitaxel (PTX 10 nM) and vincristine (VCN 5 nM). Compared to: + (control without drug), o (*βgal* without drug), # (*hIFNβ* without drug), x (*βgal* with drug), * (control with drug). 1 symbol: $P<0.05$; 2 symbols: $P<0.01$; 3 symbols: $P<0.001$.

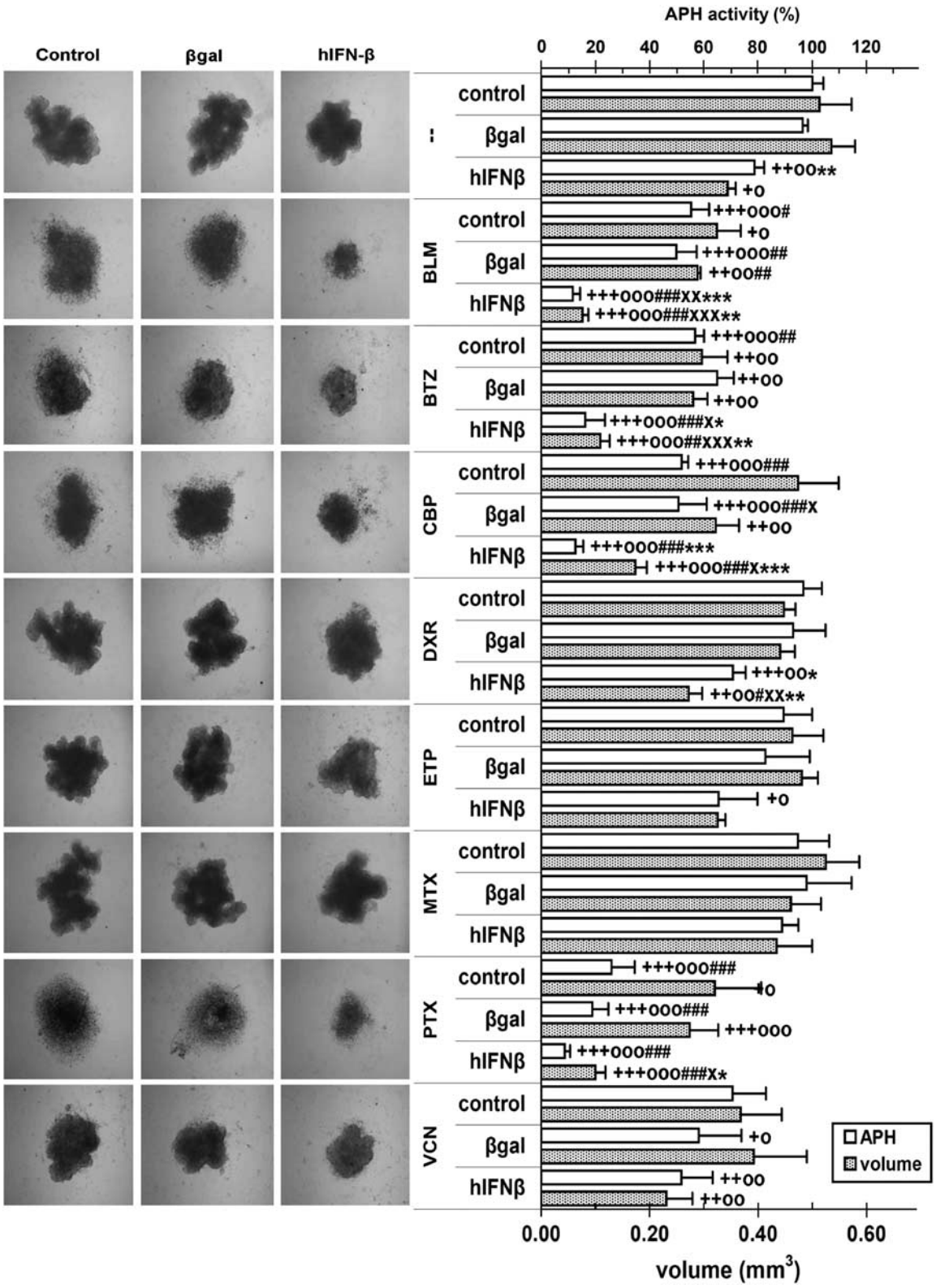

Figure 5. Responses to antineoplastic drugs for untreated (control), β-galactosidase (*βgal*)- and *hIFNβ*-lipofected M8 spheroids. The assay was performed as described in Materials and methods. Results were expressed as mean ± s.e.m. of four independent experiments. Bleomycin (BLM 10 μg ml^{-1}), bortezomib (BTZ 10 nM), carboplatin (CBP 5 μM), doxorubicin (DXR 25 ng ml^{-1}), etoposide (ETP 50 ng ml^{-1}), methotrexate (MTX 10 nM), paclitaxel (PTX 10 nM) and vincristine (VCN 5 nM). Compared to: + (control without drug), o (*βgal* without drug), # (*hIFNβ* without drug), x (*βgal* with drug), * (control with drug). 1 symbol: $P<0.05$; 2 symbols: $P<0.01$; 3 symbols: $P<0.001$.

spheroids volume as compared with their respective drug-treated controls. Conversely, *hIFNβ* lipofection resulted in a significant reduction of spheroids volume when combined with BLM, BTZ, CBP and DXR. The highest inhibitory effects were found for the combination of *hIFNβ* with BLM and BTZ as compared to drug or cytokine gene added separately. The inhibitory effects of CPT and

Table 3. IC_{50}s (μM) for antineoplastic drugs

Drug	*Treat*	*EW7*	*M8*	*Drug*	*Treat*	*EW7*	*M8*
BLM	—	3.57 ± 0.50	13.57 ± 1.43	ETP	—	0.0357 ± 0.0015	0.6167 ± 0.0595
	βgal	2.86 ± 0.43	4.29 ± 0.93		*βgal*	0.0374 ± 0.0017	0.3840 ± 0.0255
	hIFNβ	2.86 ± 0.30	2.86 ± 0.64		*hIFNβ*	0.0136 ± 0.0005	0.2939 ± 0.0255
BTZ	—	0.0042 ± 0.0002	0.0377 ± 0.0024	MTX	—	0.0060 ± 0.0003	0.0900 ± 0.0100
	βgal	0.0039 ± 0.0003	0.0215 ± 0.0038		*βgal*	0.0060 ± 0.0008	0.0340 ± 0.0013
	hIFNβ	0.0029 ± 0.0002	0.0057 ± 0.0004		*hIFNβ*	> 1	0.0370 ± 0.0015
CBP	—	7.00 ± 0.50	60.00 ± 1.00	PTX	—	0.0017 ± 0.0002	0.0044 ± 0.0004
	βgal	8.00 ± 0.70	58.00 ± 2.00		*βgal*	0.0015 ± 0.0002	0.0023 ± 0.0004
	hIFNβ	5.00 ± 0.40	8.00 ± 0.70		*hIFNβ*	0.0011 ± 0.0002	0.0022 ± 0.0005
DXR	—	0.0207 ± 0.0034	0.0828 ± 0.0045	VCN	—	0.0023 ± 0.0005	0.0700 ± 0.0030
	βgal	0.0190 ± 0.0034	0.0552 ± 0.0047		*βgal*	0.0019 ± 0.0006	0.0180 ± 0.0010
	hIFNβ	0.0155 ± 0.0017	0.0500 ± 0.0047		*hIFNβ*	0.0016 ± 0.0004	0.0080 ± 0.0003

Abbreviations: BLM, bleomycin; BTZ, bortezomib; CBP, carboplatin; DXR, doxorubicin; ETP, etoposide; MTX: methotrexate, PTX, paclitaxel; Treat, treatment; VCN, vincristine.
Values were derived from the dose–response curves displayed in Figure 3.

PTX were additive when combined with *hIFNβ* gene. Lipofection with *hIFNβ* did not modify either the inhibition of unlipofected controls caused by VCN, or the lack of effect after MTX addition.

DISCUSSION

The development of therapeutic strategies to improve overall survival in refractory advanced cancer remains a high priority.

In our study, lipofection with *hIFNβ* gene showed a stronger cytotoxic effect in human EW7 (primary) or COH (metastatic) Ewing sarcoma, and MCF-7 (mammary) tumor cells. When cultured as spheroids, most of the assayed cell lines (HT-29 excluded) manifested a relative *hIFNβ* resistance phenotype, compared with the same cells grown as sparse monolayer cultures (Figure 1). However, in every assay performed in 2D or 3D cultures (HT-29 excluded), all the *hIFNβ*-lipofected cells were significantly more sensitive than the respective *βgal*-lipofected controls (Figure 1).

Taking into account the low lipofection efficiencies of Ewing and melanoma cells (Table 1), this outcome is very encouraging. It is worth to note that the great bystander effect induced by *hIFNβ* gene lipofection could be among the main causes of its success.

The strength of the bystander effect associated with *hIFNβ* lipofection is supposed to be upregulated by mitochondrial-free radicals that could eventually diffuse or pass to adjacent unmodified tumor cells, leading them to oxidative damage.[32,33] This may allow a minimal number of hIFNβ-expressing cells (EW7: 1%, M8: 2%) to initiate the destruction of about 60 and 80% of EW7 and M8 cells, respectively. Such amplification mechanisms suggest the potential translation of the *hIFNβ* gene transfer approach as an *in vivo* therapy. In addition, our data indicate that compared to single therapy, the combination of *hIFNβ* and antineoplastic drugs may possess greater antitumor efficacy. This raises the possibility of a chemotherapy dose reduction when used in combination with gene therapy. Then, the deleterious systemic effects on normal cells could be maintained at a minimal level.

Our results, in agreement with previous studies,[19,20,24] indicate that 2D-monolayer cultures and 3D-spheroids represent two very different experimental tumor models.

Growing as monolayers, EW7 cells were always more sensitive than M8 to increasing concentrations of antineoplastic drugs, and M8 cells were more sensitive to *hIFNβ* lipofection. Assembled as spheroids, M8 cells were sensitive and EW7 resistant to BLM, BTZ and PTX, while EW7 cells were sensitive and M8 resistant to DXR, MTX and VCN. In addition, both EW7 and M8 control spheroids were sensitive to CBP and resistant to ETP.

On the other hand, while M8 cells manifested a relative MCR phenotype to *hIFNβ* gene therapy when growing as spheroids, compared with the same cells growing as sparse monolayers, EW7 cells displayed similar sensitivity in any culture configuration.

As seen in Figures 4 and 5, in the absence or presence of antineoplastic drugs, EW7 and M8 spheroids were not sensitive to *βgal* lipofection, but they were sensitive to *hIFNβ* that caused about 50 and 30% of spheroid volume loss, respectively. When combined with antineoplastic agents, *hIFNβ* lipofection displayed additive (CBP, DXR, PTX and VCN) or strongly enhanced effects (BLM, BTZ) as compared with drug or the cytokine genes added separately.

It is worth to note that, although the spheroids were either resistant (EW7) or sensitive (M8) to single drug treatment such as BLM, BTZ or PTX, when combined with *IFNβ* gene therapy they reached similar final effects (additive: PTX or enhanced: BLM, BTZ). On the other hand, spheroids of EW7 (sensitive to MTX) or M8 (resistant to MTX) displayed counteractive (EW7) or no effects (M8) when combined with *hIFNβ*. In addition, EW7 and M8 spheroids both highly sensitive to CBP, displayed additive (EW7) or potentiated effects (M8) when combined with *hIFNβ* gene lipofection.

Although we assayed drugs aimed at diverse cell targets, we found an underlying common mechanism. In cells that manifested a relative MCR phenotype to *hIFNβ* gene (M8 spheroids) or drugs (M8 monolayers and EW7 spheroids), the combination of *hIFNβ* gene therapy with drugs that mainly operate at the genotoxic level (MTX, DXR, PTX) presented additive effects. However, drugs that additionally increased pro-oxidant species (BLM, BTZ, CBP, ETP, VCN)[34–38] were able to complement the antitumor efficacy of the *hIFNβ* gene and clearly caused strongly enhanced effects. These results are in agreement with the fact that the great bystander effect of the *hIFNβ* gene lipofection involves the production of reactive oxygen species, simultaneous with a mitochondrial potential decrease in both cell lines.[39]

The combination antineoplastic drug/*hIFNβ* gene in the chemotherapy-sensitive cells (monolayers of EW7) displayed only additive or counteractive effects. This suggests that, when cells do not exhibit resistance, the cytotoxic mechanisms triggered by *hIFNβ* gene lipofection may be saturating the signaling pathways. Thus, the addition of drugs did not enhance the effect. Conversely, when EW7 displayed resistance (cultured as spheroids), strong enhanced effects appeared in 50% of the combinations (BLM, BTZ, ETP, VCN), as it happened in the monolayers of the chemotherapy-resistant M8 melanoma tumor cell line (BLM, BTZ, CBP, VCN).

Collectively, our data indicate that *in vitro* sensitivity of cells to *hIFNβ* gene/chemotherapeutic drugs combined therapy depends on the expression of a resistance phenotype rather than on the origin of the tumor cells. In addition, the sensitivity or resistance to drug or *hIFNβ* gene added separately does not allow predicting the effects of the combination, when the great bystander effect

induced by *hIFNβ* gene could be amplified by the production of reactive oxygen species. The effect of added antioxidants that could diminish or prevent this phenomenon is currently being investigated by our laboratory.

All these observations demonstrate that, compared with single therapy, the combination of *hIFNβ* gene therapy and neoplastic drugs may possess greater antitumor efficacy and encourage the development of specific probes on spheroids of each tumor system, which represent more closely the *in vivo* situation of tumor cells, supporting the development of *in vivo* complementary studies for further characterization of the proposed combined approaches.

CONFLICT OF INTEREST

The authors declare no conflict of interest.

ACKNOWLEDGEMENTS

We thank Dr Susanna Kevra for critical reading of the manuscript, Dr Juana Wietzerbin for EW7 and COH cells, and Ana Bihary and Graciela Zenobi for technical assistance. This study was partially supported by grants from ANPCYT/FONCYT (PICT 2002-12084 and PICT 2007-00539) and UBA (PID-UBACYT-2008/2010-M027). GCG and LMEF are investigators, and MSV and MLG-C are fellows of the Consejo Nacional de Investigaciones Científicas y Técnicas (CONICET, Argentina).

REFERENCES

1 Kurzrock R, Talpaz M, Gutterman JU. Hairy cell leukaemia: review of treatment. *Br J Haematol* 1991; **79**: 17–20.
2 Gutterman JU. Cytokine therapeutics: lessons from interferon alpha. *Proc Natl Acad Sci USA* 1994; **91**: 1198–1205.
3 Borden EC. Gene regulation and clinical roles for interferons in neoplastic diseases. *Oncologist* 1998; **3**: 198–203.
4 Talpaz M. Interferon-alfa-based treatment of chronic myeloid leukemia and implications of signal transduction inhibition. *Semin Hematol* 2001; **38**: 22–27.
5 Sherwin SA, Knost JA, Fein S, Abrams PG, Foon KA, Ochs JJ *et al.* A multiple-dose phase I trial of recombinant leukocyte A interferon in cancer patients. *JAMA* 1982; **248**: 2461–2466.
6 Wadler S, Schwartz EL. Antineoplastic activity of the combination of interferon and cytotoxic agents against experimental and human malignancies: a review. *Cancer Res* 1990; **50**: 3473–3486.
7 Daponte A, Ascierto PA, Gravina A, Lelucci MT, Palmieri G, Comella P *et al.* Cisplatin, dacarbazine, and fotemustine plus interferon alpha in patients with advanced malignant melanoma. A multicenter phase II study of the Italian Cooperative Oncology Group. *Cancer* 2000; **89**: 2630–2636.
8 Atzpodien J, Neuber K, Kamanabrou D, Fluck M, Brocker EB, Neumann C *et al.* Combination chemotherapy with or without s.c. IL-2 and IFN-alpha: results of a prospectively randomized trial of the Cooperative Advanced Malignant Melanoma Chemoimmunotherapy Group (ACIMM). *Br J Cancer* 2002; **86**: 179–184.
9 Salmon P, Le Cotonnec JY, Galazka A, Abdul-Ahad A, Darragh A. Pharmacokinetics and pharmacodynamics of recombinant human interferon-beta in healthy male volunteers. *J Interferon Cytokine Res* 1996; **16**: 759–764.
10 Finocchiaro LME, Villaverde MS, Gil Cardeza ML, Riveros MD, Glikin GC. Cytokine-enhanced vaccine and interferon-β plus suicide gene as combined therapy for spontaneous canine sarcomas. *Res Vet Sci* 2011; **91**: 230–234.
11 Matsumoto K, Kubo H, Murata H, Uhara H, Takata M, Shibata S *et al.* A pilot study of human interferon beta gene therapy for patients with advanced melanoma by *in vivo* transduction using cationic liposomes. *Jpn J Clin Oncol* 2008; **38**: 849–856.
12 Yoshida J, Mizuno M, Wakabayashi T. Interferon-β gene therapy for cancer: basic research to clinical application. *Cancer Sci* 2004; **95**: 858–865.
13 Papageorgiou A, Kamat A, Benedict WF, Dinney C, McConkey DJ. Combination therapy with IFN-alpha plus bortezomib induces apoptosis and inhibits angiogenesis in human bladder cancer cells. *Mol Cancer Ther* 2006; **5**: 3032–3041.
14 Shieh GS, Shiau AL, Yo YT, Lin PR, Chang CC, Tzai TS *et al.* Low-dose etoposide enhances telomerase-dependent adenovirus-mediated cytosine deaminase gene therapy through augmentation of adenoviral infection and transgene expression in a syngeneic bladder tumor model. *Cancer Res* 2006; **66**: 9957–9966.
15 Deharvengt S, Rejiba S, Wack S, Aprahamian M, Hajri A. Efficient electrogene therapy for pancreatic adenocarcinoma treatment using the bacterial purine nucleoside phosphorylase suicide gene with fludarabine. *Int J Oncol* 2007; **30**: 1397–1406.
16 Abaza MS, Al-Saffar A, Al-Sawan S, Al-Attiyah R. c-myc antisense oligonucleotides sensitize human colorectal cancer cells to chemotherapeutic drugs. *Tumour Biol* 2008; **29**: 287–303.
17 Fandy TE, Shankar S, Srivastava RK. Smac/DIABLO enhances the therapeutic potential of chemotherapeutic drugs and irradiation, and sensitizes TRAIL-resistant breast cancer cells. *Mol Cancer* 2008; **7**: 60.
18 Fridlender ZG, Sun J, Singhal S, Kapoor V, Cheng G, Suzuki E *et al.* Chemotherapy delivered after viral immunogene therapy augments antitumor efficacy via multiple immune-mediated mechanisms. *Mol Ther* 2010; **18**: 1947–1959.
19 Finocchiaro LME, Bumaschny VF, Karara AL, Fiszman GL, Casais CC, Glikin GC. Herpes simplex virus thymidine kinase/ganciclovir system in multicellular tumor spheroids. *Cancer Gene Ther* 2004; **11**: 333–345.
20 Gil Cardeza ML, Villaverde MS, Fiszman GL, Altamirano NA, Cwirenbaum RA, Glikin GC *et al.* Suicide gene therapy on spontaneous canine melanoma: correlations between *in vivo* tumors and their derived multicell spheroids *in vitro*. *Gene Therapy* 2010; **17**: 26–36.
21 Sancéau J, Poupon MF, Delattre O, Sastre-Garau X, Wietzerbin J. Strong inhibition of Ewing tumor xenograft growth by combination of human interferon-alpha or interferon-beta with ifosfamide. *Oncogene* 2002; **21**: 7700–7709.
22 Gnjatic S, Cai Z, Viguier M, Chouaib S, Guillet JG, Choppin J. Accumulation of the p53 protein allows recognition by human CTL of a wild-type p53 epitope presented by breast carcinomas and melanomas. *J Immunol* 1998; **160**: 328–333.
23 Finocchiaro LME, Glikin GC. Cytokine-enhanced vaccine and suicide gene therapy as surgery adjuvant treatments for spontaneous canine melanoma. *Gene Therapy* 2008; **15**: 267–276.
24 Casais CC, Karara AL, Glikin GC, Finocchiaro LME. Effects of spatial configuration on tumor cells transgene expression. *Gene Ther Mol Biol* 2006; **10**: 207–222.
25 Felgner JH, Kumar R, Sridhar CN, Wheeler CJ, Tsai YJ, Border R *et al.* Enhanced gene delivery and mechanism studies with a novel series of cationic lipid formulations. *J Biol Chem* 1994; **269**: 2550–2561.
26 Gao X, Huang L. Cationic liposome-mediated gene transfer. *Gene Therapy* 1995; **2**: 710–722.
27 Friedrich J, Eder W, Castaneda J, Doss M, Huber E, Ebner R *et al.* A reliable tool to determine cell viability in complex 3-d culture: the acid phosphatase assay. *J Biomol Screen* 2007; **12**: 925–937.
28 Bradford MM. A rapid and sensitive method for the quantitation of microgram quantities of protein utilizing the principle of protein-dye binding. *Anal Biochem* 1976; **72**: 248–254.
29 Li S, Wilkinson M, Xia X, David M, Xu L, Purkel-Sutton A *et al.* Induction of IFN-regulated factors and antitumoral surveillance by transfected placebo plasmid DNA. *Mol Ther* 2005; **11**: 112–119.
30 Boyd M, Mairs SC, Stevenson K, Livingstone A, Clark AM, Ross SC *et al.* Transfectant mosaic spheroids: a new model for evaluation of tumour cell killing in targeted radiotherapy and experimental gene therapy. *J Gene Med* 2002; **4**: 567–576.
31 Kostarelos K, Emfietzoglou D, Papakostas A, Yang WH, Ballangrud A, Sgouros G. Binding and interstitial penetration of liposomes within avascular tumor spheroids. *Int J Cancer* 2004; **112**: 713–721.
32 Huang G, Chen Y, Lu H, Cao X. Coupling mitochondrial respiratory chain to cell death: an essential role of mitochondrial complex I in the interferon-beta and retinoic acid-induced cancer cell death. *Cell Death Differ* 2007; **14**: 327–337.
33 Kagan VE, Bayir HA, Belikova NA, Kapralov O, Tyurina YY, Tyurin VA *et al.* Cytochrome c/cardiolipin relations in mitochondria: a kiss of death. *Free Radic Biol Med* 2009; **46**: 1439–1453.
34 Burger RM. Cleavage of nucleic acids by bleomycin. *Chem Rev* 1998; **98**: 1153–1170.
35 Husain K, Whitworth C, Somani SM, Rybak LP. Carboplatin-induced oxidative stress in rat cochlea. *Hearing Res* 2001; **159**: 14–22.
36 Kagan VE, Kuzmenko AI, Tyurina YY, Shvedova AA, Matsura T, Yalowich JC. Pro-oxidant and antioxidant mechanisms of etoposide in HL-60 cells. *Cancer Res* 2001; **61**: 7777–7784.
37 Olszewska-Słonina DM, Styczyński J, Czajkowski R, Drewa TA, Musiałkiewicz D. Cell cycle, melanin contents and apoptosis processes in B16 and Cloudman S91 mouse melanoma cells after exposure to cytostatic drugs. *Acta Pol Pharm* 2007; **64**: 469–478.
38 Du ZX, Zhang HY, Meng X, Guan Y, Wang HQ. Role of oxidative stress and intracellular glutathione in the sensitivity to apoptosis induced by proteasome inhibitor in thyroid cancer cells. *BMC Cancer* 2009; **9**: 56.
39 Villaverde MS, Gil-Cardeza ML, Glikin GC, Finocchiaro LME. Mechanisms involved in cell death and bystander effect induced by cationic lipid mediated interferon-β gene transfer to human tumor cells. *Cancer Gene Ther* 2012; **19**: 420–430.